Reactive epitaxial growth of MnSi ultrathin films on Si(111) by Mn deposition

Shougo Higashi,[1] Pavel Kocán,[1,2] and Hiroshi Tochihara[1,*]
[1]*Department of Molecular and Material Sciences, Kyushu University, Kasuga, Fukuoka 816-8580, Japan*
[2]*Department of Surface and Plasma Science, Faculty of Mathematics and Physics, Charles University in Prague, V Holešovičkách 2, 180 00 Praha 8, Czech Republic*

(Received 8 December 2008; revised manuscript received 10 April 2009; published 13 May 2009)

Manganese (Mn) adsorption on the Si(111)-(7×7) surface followed by annealing at a relatively low temperature of 250 °C has been studied by using scanning tunneling microscopy as well as low-energy electron diffraction and Auger-electron spectroscopy. The B20-type structure of a Mn monosilicide (MnSi) of epitaxial ultrathin films is formed with a $(\sqrt{3}\times\sqrt{3})$R30° periodicity. Morphologies of the crystalline MnSi ultrathin films have been investigated for Mn coverage of 1.5, 3, and 5 monolayers (ML). We found a characteristic mode of crystal growth for compound formation in the solid-on-solid system. At each amount of the Mn deposition, structural features, morphology, and formation processes of the MnSi films can be explained by the mass balance between deposited Mn and usable Si atoms. We found that the epitaxial MnSi ultrathin films can be grown coherently on Si(111) at 3 ML of Mn deposition. At 5 ML, the supply of Si atoms from bulk to surface becomes significant, then many deep holes are formed and the surface morphology becomes rough. It is found that the codeposition of Mn and Si leads to the formation of anomalously smooth MnSi surfaces.

DOI: 10.1103/PhysRevB.79.205312 PACS number(s): 68.55.−a, 68.37.−d

I. INTRODUCTION

Fabrication of ferromagnetic (FM) layer onto semiconductor surfaces has received a considerable attention because of its potential application to information processing devices utilizing the spin of electron,[1] categorized as spintronics.[2] Accomplishment of an efficient injection of spin polarized current from FM layers into semiconductors is one of major challenges to realize practical devices. So far, several investigations have been conducted on the growth of FM transition metals or metal silicide films on semiconductors.[3–6] However, studies concerned with FM films on silicon surfaces, which are widely used in semiconductor industry, are few and the film required as the efficient spin injector has not been reported yet. Among systems of transition-metal silicides on Si surfaces, MnSi is considered to be a good candidate as a spin injector since it exhibits the ferromagnetism in the bulk. In addition, it was reported that ultrathin MnSi films formed on the Si(111) surface have a spin polarization of 50% at the Fermi level by calculations using density-functional theory (DFT).[7] It was also demonstrated that Mn atoms at the surface and interface possess large magnetic moments. Therefore, the MnSi ultrathin film on Si(111) would be a promising material for Si-based spintronics.

Experimentally, Mn deposition on the Si(111)-(7×7) surface has been studied by several groups but most studies reported so far are on the formation of three-dimensional (3D) islands or on very initial processes of Mn deposition on the surface.[8–10] At 1 monolayer (ML; 1 ML=7.83×10^{14} atoms/cm^2) deposition, Evans *et al.*[11] observed by using scanning tunneling microscopy (STM) tabular islands with a $(\sqrt{3}\times\sqrt{3})$R30° termination interrupted by bare Si surface at annealing temperatures between 325 °C and 450 °C. Nagao *et al.*[13] found such islands ranging up to several hundreds of angstroms with various heights depending on the annealing temperature. Kumar *et al.*[12] observed that with increasing coverage to 5 ML such islands almost close the bare Si surface at 400 °C, leading to patched films with various heights as well as deep holes. So far, the annealing was done under relatively high temperatures in most studies.[11–13] Recently, Hortamani *et al.*[7] showed by using DFT calculations that the B20-type structure (bulk crystal structure) of the MnSi, whose (111) plane coincides with the $(\sqrt{3}\times\sqrt{3})$R30° lattice of the Si(111) plane with a mismatch of 3.2%, is more stable than the pseudomorphic B2 (CsCl-type structure). Ball model of the B20-type structure is depicted in Fig. 1. The validity of the assignment of the B20-type MnSi structure formed on Si(111) is recently confirmed by means of surface x-ray diffraction analysis using synchrotron radiation.[14]

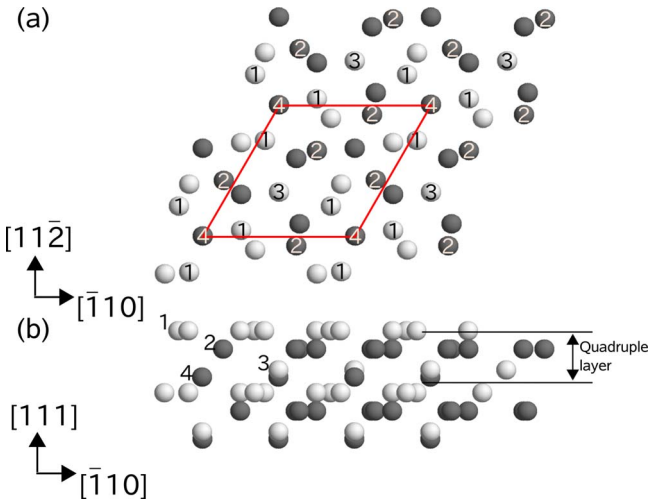

FIG. 1. (Color online) Ball model of the B20-type structure of MnSi for (a) top view and (b) side view. White balls represent Si atoms and dark balls Mn atoms. In (a), a unit mesh of $(\sqrt{3}\times\sqrt{3})$R30° with respect to the Si(111) is outlined. In (b), it is shown that 1 QL consists of four different layers (numbered 1–4). In (a), all atoms located in the four different layers are numbered from 1 to 4 only for the top QL according to the numbers in (b).

Very recently, we have reported a recipe for the epitaxial growth of flat MnSi ultrathin films on Si(111).[15] As the spin injector, atomic flatness of an interface between Si substrate and FM films is crucial to minimize scattering from defects and/or impurity states. We can expect the formation of flat interfaces between the MnSi and the Si(111) substrate if the surfaces of the MnSi films are atomically smooth. The recipe is simple: after deposition of Mn atoms of 3 ML on the Si(111)-(7×7) surface at room temperature (RT) the sample is annealed at a relatively low temperature of 250 °C for more than 5 min.

In this paper, in order to know the reason why the 3 ML-Mn deposition is the appropriate condition to form the flat MnSi ultrathin films at 250 °C annealing, we have investigated STM images of surfaces where Mn atoms are deposited by 1.5, 3, and 5 ML. In addition we have studied the effect of annealing time. Detailed investigation led to proposal of another mode of crystal growth and to understanding of the formation processes of the MnSi ultrathin films. We have tried another procedure for producing flat MnSi ultrathin films. That is, not only Mn but Si atoms are deposited on the Si(111)-(7×7) surface (denoted codeposition) then the surface is annealed at 250 °C. This procedure produces anomalously flat surfaces of the MnSi films.

After the description of experimental part in Sec. II, results of low-energy electron-diffraction (LEED) intensity measurement and Auger-electron spectroscopy (AES) are briefly mentioned in Sec. III. Then, STM images taken at 1.5, 3, and 5 ML are separately presented with detailed discussion in Sec. IV. In Sec. V, the formation processes of the MnSi ultrathin films are discussed based on the results obtained mainly by STM measurements. We show the STM images of surfaces prepared by codeposition of Mn and Si in Sec. VI. Finally, we summarize our experimental results and the essence of the formation processes of the MnSi films.

II. EXPERIMENT

Experiments were carried out in an ultrahigh-vacuum system consisting of a sample preparation chamber with LEED and a chamber for STM measurement. The base pressures of both chambers were about 1×10^{-10} Torr. Clean surfaces were accomplished by flashing samples at 1200 °C for a few seconds several times, with subsequent annealing at 700 °C for 5 min and cooling down to RT with a rate of 10 °C/s in order to prepare large terraces of (7×7). The surface quality was checked by observing clear and sharp (7×7) LEED patterns. Mn was evaporated from a homemade Knudsen cell by resistive heating[16] and Si deposition was carried out by passing dc directly to a piece of Si wafer (10×2 mm^2). The calibration of deposited amounts was performed using a crystal thickness monitor and the deposition rates of Mn and Si were estimated to be ~0.3 and ~0.6 ML/min, respectively. Sample temperature was kept at RT and pressures during deposition were less than 3×10^{-10} Torr. After the deposition, the sample was annealed at 250 °C for several minutes. The temperature was measured with an infrared pyrometer. The AES was measured by using a four-grid LEED optics. Intensities of LEED spots were measured with a high sensitive charge-coupled device (CCD) camera at RT. After annealing, the samples were transferred to the STM chamber and the structure and morphology were investigated by STM (Unisoku, USM-901) at RT.

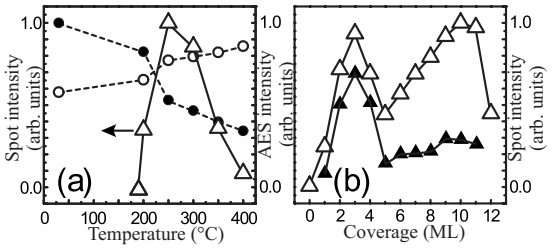

FIG. 2. (a) Intensity change of (1/3 1/3) LEED spots as a function of annealing temperature (triangles). AES intensities of Mn (40 eV, filled circles) and Si (92 eV, open circles) are plotted against annealing temperature. 3 ML Mn was deposited at RT. Incident electron energies for LEED and AES are 115 eV and 1 keV, respectively. (b) Intensity change of (1/3 1/3) LEED spots at incident energy of 115 (open triangle) and 173 (filled triangle) eV as a function of Mn coverage. Samples were annealed at 250 °C for 5 min.

III. LEED SPOT INTENSITY AND AES MEASUREMENTS

LEED intensities of (1/3 1/3) spots reflecting the area of ordered MnSi domains with the $(\sqrt{3}\times\sqrt{3})$R30° periodicity are shown in Fig. 2(a) as a function of annealing temperature between 185 °C and 400 °C (annealing time is 5 min). The amount of deposited Mn was ~3 ML. AES intensities of Mn (40 eV, filled circle) and Si (92 eV, open circle) are also plotted in Fig. 2(a). AES intensity of Mn decreased steeply between 200 °C and 250 °C, while that of Si considerably increased. The changes in the AES intensities suggest that vertical mass transfer of Si atoms takes place efficiently around 250 °C. In accordance with the AES changes, the LEED intensity steeply increases between 200 °C and 250 °C and reaches a maximum at 250 °C. Then, it decreases rapidly above 300 °C. The decrease reflects a change in morphology from the MnSi two-dimensional (2D) islands to 3D islands.[11] Thus, at 250 °C the MnSi films are most extensively formed on the surfaces. In Fig. 2(b), LEED intensities of the (1/3 1/3) spots at incident energies of 115 (open triangle) and 173 (filled triangle) eV are plotted as a function of Mn coverage. Mn deposited surfaces were annealed at 250 °C for 5 min for each measurement. At both energies, the intensities exhibit sharp maxima at 3 ML, where the area of the ordered MnSi is the widest. More deposition of Mn than 3 ML leads to a decrease in the ordered area of the MnSi. Thus, the MnSi thin film grows most extensively at 3 ML of Mn deposition and subsequent annealing at 250 °C. In the next section, we see how the surface morphology changes with increase in Mn coverage and in annealing time by observing STM images.

IV. INDIVIDUAL DEPOSITION OF Mn ON Si(111)

A. 1.5 ML-Mn deposition followed by annealing

Figures 3(a) and 3(b) show STM images of 1.5-ML-Mn-deposited surfaces followed by annealing at 250 °C for 5

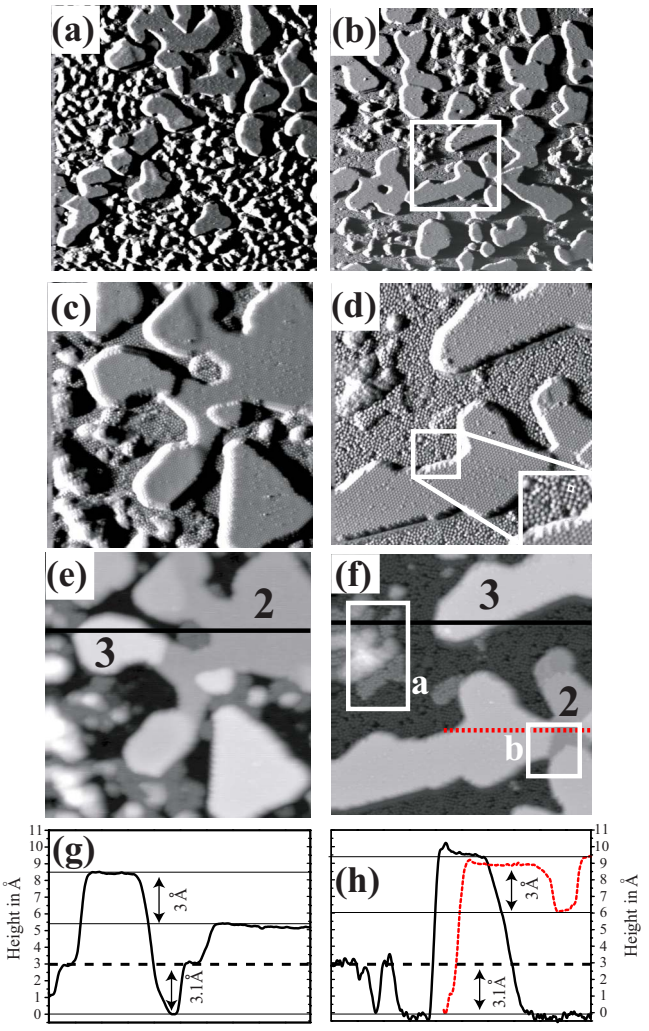

FIG. 3. (Color online) STM images of 1.5-ML-Mn-deposited surfaces followed by annealing at 250 °C. Annealing times for (a) and (b) are 5 and 30 min, respectively, and both imaging areas are 150×150 nm^2. (a)–(d) are CH mode images with sample bias (V_S) of 1.5 V. (c)–(f) are magnified images of 60×60 nm^2. (d) is a magnified image of the outlined region in (b). (e) and (f) are CC mode images of (c) and (d), respectively. The numbers in (e) and (f) indicate height of the grown MnSi 2D islands in unit of QL. Regions a and b in (f) are magnified in Figs. 4(a) and 4(b), respectively. (g) and (h) show profiles along lines in (e) and (f), respectively. The original level of the Si(111)-(7×7) is shown by dashed line.

and 30 min, respectively. Both areas are 150×150 nm^2 but probing sites are not identical. Figures 3(a) and 3(b) are constant-height (CH) mode images. In the present study we used a sample bias (V_S) of 1.5 V otherwise noted. In Fig. 3(a) there are many irregular clusters in addition to small 2D islands and the former almost disappears after 30 min annealing in Fig. 3(b). It is noted that Mn deposition of 1.5 ML at RT led to the appearance of a range of "hillock" in STM images (not shown here).[11] Therefore, we conclude that the irregular clusters in Fig. 3(a) consist of Mn atoms. In Fig. 3(b), in addition to the grown 2D islands, relatively large areas of bare Si(111) surfaces can be seen (denoted "craters" hereafter).

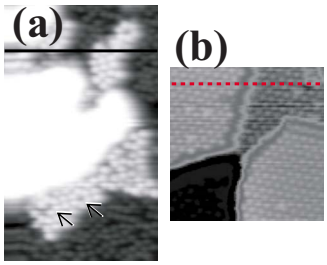

FIG. 4. (Color online) (a) and (b) are magnified CC mode images from regions a and b in Fig. 3(f), respectively. In (a) arrows indicate corner holes on the (7×7) reconstruction in survived area. White area is an unknown structure, probably unreacted Mn cluster. Contrast in (b) is nonlinearly enhanced to show the structure of different levels of the MnSi.

A clear image of the crater is shown in a magnified image of Fig. 3(d) from an outlined region in Fig. 3(b). The inset in Fig. 3(d) clearly shows that the surface of the craters is decorated by Si adatoms[11] which are arranged to be a rather disordered (2×2) [denoted "2×2" hereafter]. Figure 3(c) is a similarly magnified image from the surface after 5 min annealing but its location is not within Fig. 3(a). Figures 3(e) and 3(f) correspond to constant-current (CC) mode images of Figs. 3(c) and 3(d), respectively. A further enlarged STM image of region *a* outlined in Fig. 3(f) is shown in Fig. 4(a). We can recognize narrow areas of survivals of the original Si(111) surface: corner holes being specific to the (7×7) reconstruction can be seen as shown by arrows. Thus, we assign that the height difference between the survived narrow areas and the craters is the thickness of 1 bilayer (BL) of the Si(111) plane, 3.1 Å. This value is used as a height standard in line profiles in Figs. 3(g) and 3(h). The height of the original Si(111)-(7×7) surface is depicted by a dashed line in Figs. 3(g) and 3(h).

Along a dotted line in Fig. 3(f) the tip scans a higher and a lower level of a 2D island. Its profile is shown in Fig. 3(h) as a dotted line. The height difference between the higher and lower levels is derived to be ~3 Å, which is practically in good agreement with a stacking-unit distance of the B20-type MnSi crystal along the [111] direction. We call the unit 1 quadruple layer (QL) (see Fig. 1, strictly its thickness is 2.7 Å in the bulk structure). One QL consists of the so-called Si sparse, Mn sparse, Si dense, and Mn dense layers[7] and atoms in each layer are marked with numbers 1–4, respectively, as shown in Fig. 1. The interlayer distance of ~3 Å has been also confirmed in Fig. 3(g) as well as on several 2D islands. Therefore, we suggest that the grown 2D islands are the B20-type MnSi and that the MnSi islands grow with the thickness unit of 1 QL. Figure 4(b), being magnified from outlined square *b* in Fig. 3(f), shows that both higher and lower levels of the 2D island exhibit the $(\sqrt{3}\times\sqrt{3})$R30° arrangement of protrusions. In order to know clearly the relation of the arrangement of the protrusions between the two layers with the height difference of 1 QL, we show another CC mode image around the two-level structure in Fig. 5(a). A hexagonal grid of the $(\sqrt{3}\times\sqrt{3})$R30° order is partially overlaid on the image. It is found that on the lower level the protrusions are located at centers of triangles in the

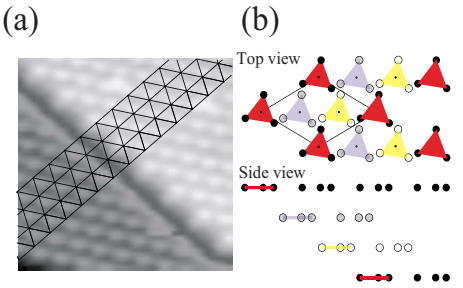

FIG. 5. (Color online) CC mode image (60×60 nm^2) around two-level structure (height difference corresponds to 1 QL). A single triangular mesh of the $(\sqrt{3}\times\sqrt{3})$R30° is overlaid partially. (b) Schematic top and side views of consecutive 3 QLs, in which a Si-dense layer represents each QL for simplicity: filled, gray, and open circles represent Si atoms in the top, second, and third QLs, respectively, as seen in a side view. Three nearby Si atoms (hatched triangle in top view) is assumed to exhibit one protrusion in STM image in (a). A parallelogram is a unit mesh of $(\sqrt{3}\times\sqrt{3})$R30° with respect to the Si(111). Contrast in (a) is nonlinearly enhanced to show the structure of different levels of the MnSi.

grid while they are at corners of the triangles on the higher level. This is consistent with the B20-type MnSi structure schematically shown in Fig. 5(b). We do not know which layer appears on the top of each QL among the four different layers at this moment, but we assume here it is the dense Si layer. (Even if we choose other layers, the discussion below is the same.) So only atoms in the Si-dense layer of three consecutive QLs are depicted in Fig. 5(b) for simplicity: filled, gray, and open circles represent Si atoms in the top, second, and third QLs, respectively, as seen in a side view. Three nearby Si atoms [a hatched triangle in top view of Fig. 5(b)] is assumed to exhibit one protrusion in STM images in Fig. 5(a). Atoms in the lower QL are shifted by 4 Å along a long diagonal of a parallelogram. This is in agreement with the observed shift of the protrusions in Fig. 5(a). Thus it is supported again that the grown MnSi is the B20-type structure and that the MnSi films grow with a unit of 1 QL.

In several CC mode images after 30 min annealing we measured fractions of area of the higher and lower levels of the MnSi, obtaining 20% and 30%, respectively on average. Recalling the density of Mn in 1 QL is 4/3 ML, we can calculate approximate amount of Mn in the islands. Assuming the thickness of the lower level in Fig. 3(f) as 2 QLs, we obtain a total amount of 1.6 ML of Mn, which practically agrees with the value measured by the crystal monitor, 1.5 ML. If we assume that the lower level is 1 or 3 QLs, then the amount of Mn in the MnSi islands is 0.9 or 2.7 ML. Therefore, we exclude the two possible thicknesses. Thus, we assign the levels marked 2 and 3 in Figs. 3(e) and 3(f) as the second and the third QLs of the MnSi 2D islands, respectively. 2D islands with a thickness of 1 QL have never been found in the present studies.

B. 3 ML-Mn deposition followed by annealing

3 ML-Mn deposition with subsequent annealing at 250 °C results in transformation of almost entire surface into the flat MnSi films as shown in Figs. 6(a) and 6(b), which are

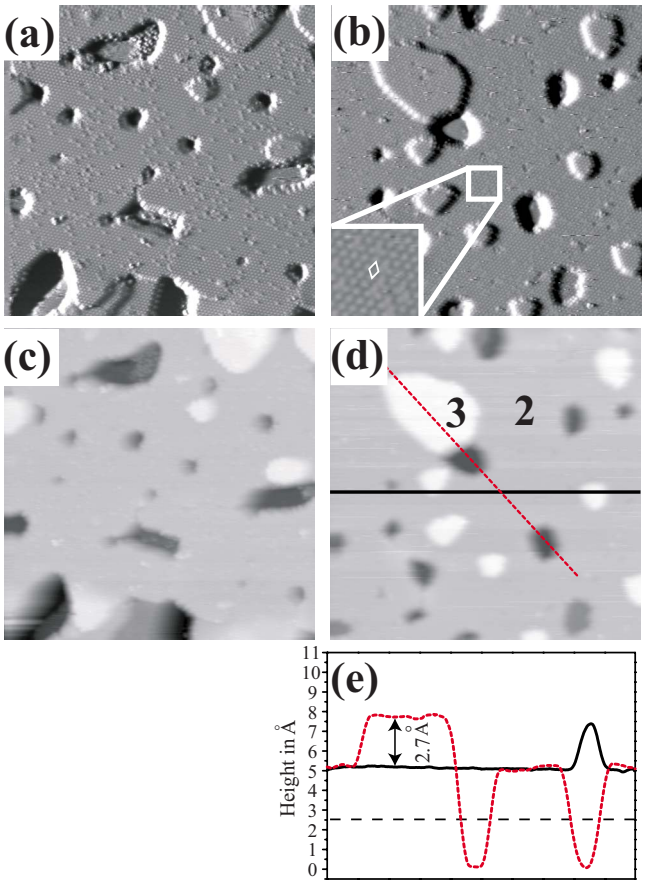

FIG. 6. (Color online) STM images of samples prepared by deposition of 3 ML of Mn followed by annealing at 250 °C. (a) and (b) constant-height mode images at annealing time of 5 and 30 min, respectively. (c) and (d) constant-current mode images of (a) and (b), respectively. All images are taken at $V_S=-1.0$ V with 50×50 nm^2. In (d), numbers 2 and 3 mark second and third QLs of MnSi film, respectively. (e) Profiles along lines in (d). Dashed line indicates the original surface level.

CH mode images after 5 and 30 min annealing, respectively. Corresponding CC mode images are presented in Figs. 6(c) and 6(d), respectively. There occur no significant morphological changes caused by annealing time, but we note that larger holes observed at 5 min annealing change to small ones at 30 min. About 80% of the surface is covered by the atomically flat MnSi films. A magnified image is shown at the bottom left of Fig. 6(b), indicating the $(\sqrt{3}\times\sqrt{3})$R30° arrangement of the protrusions. In CC mode images there exist some small white 2D islands on the flat surface (~15% of the whole surface). According to the conclusion in the case of 1.5 ML-Mn, the white islands are higher by 1 QL than the flat area. Thus, we assigned that the height difference between the lower and higher levels is 2.7 Å and it is used as a height standard in Fig. 6. We suggest that the flat area is the second QL: the total amount of Mn atoms in the films can be estimated to be $(0.8\times2\times\frac{4}{3}+0.15\times3\times\frac{4}{3})$ =2.7 ML from the area percentages and Mn coverage mentioned above. This is in good agreement with the value measured by the crystal monitor, ~3 ML. Thus, we conclude that almost complete MnSi films of 2 QLs are formed by 3

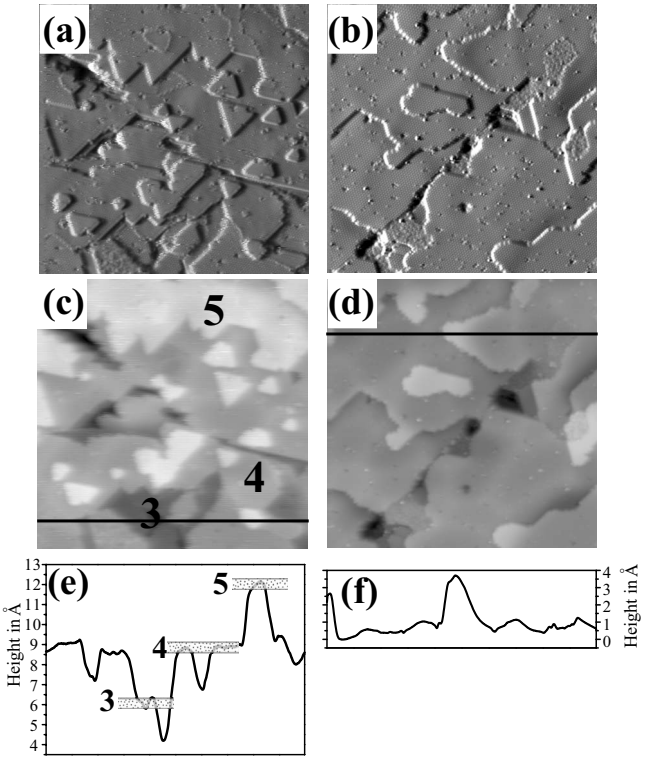

FIG. 7. STM images of samples prepared by depositing 5 ML of Mn followed by annealing at 250 °C. (a) and (b) constant-height mode images at annealing time of 5 and 30 min, respectively. V_S=1.0 V. (c) and (d) constant-current mode images of (a) and (b), respectively. All images are 60×60 nm^2. (e) and (f) are profiles along lines in (c) and (d), respectively. In (c) and (e), numbers 3, 4, and 5 mark third, fourth, and fifth QLs of MnSi film, respectively.

ML-Mn deposition and subsequent annealing at 250 °C. It is noted that such atomically flat MnSi surfaces can be formed only at ~3 ML deposition under the condition of postannealing at 250 °C. In accordance with STM observations, LEED spot intensity of the third order against the amount of deposited Mn in Fig. 2(b) indicates that the MnSi films grow most extensively at 3 ML. If we raise the annealing temperature higher than 300 °C, the flat MnSi films convert to 3D islands as indicated in the decrease in the spot intensity in Fig. 2(a). As another feature in Fig. 6, there exist small holes with diameters of 1.5–6 nm in Fig. 6(d). These holes reach deeper levels than the original surface as seen along a dotted-line profile in Fig. 6(e). Later we discuss the relationship between the holes and the grown MnSi.

C. 5 ML-Mn deposition followed by annealing

Deposition of 5 ML-Mn and subsequent annealing at 250 °C for 5 min led to the formation of uneven surfaces as shown in Fig. 7(a), contrary to the case of 3 ML deposition. The corresponding CC mode image is shown in Fig. 7(c). As in the case of 3 ML-Mn deposition, holes are observed. Referring a line profile in Fig. 7(e) taken along a solid line in Fig. 7(c), we can distinguish three layers with a height difference of 1 QL thickness (hatched three bars). We assign that the highest layer [white area in Fig. 7(c)] is the fifth QL.

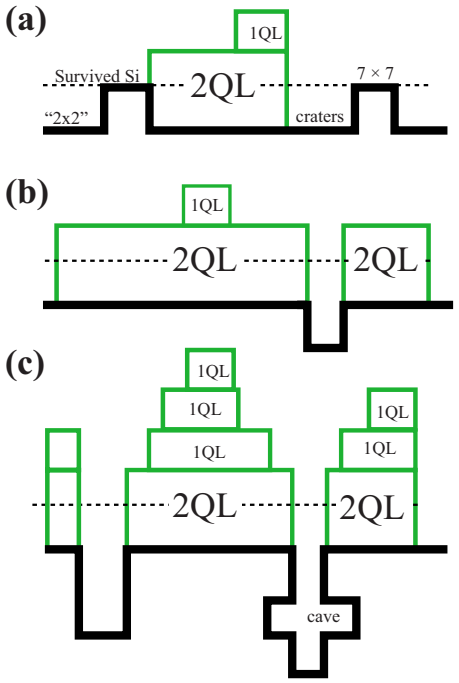

FIG. 8. (Color online) Schematic cross sectional views of (a) 1.5, (b) 3, and (c) 5-ML-Mn deposited surfaces followed by annealing at 250 °C. 2 QLs of the MnSi film appearing at the initial growth are shown. Thick lines indicate the bare Si surface and interface. Dotted lines show the level of original surface of the (7×7) reconstruction.

The fourth and the third QLs are numbered as well. The assignment of the layer number is not evidenced by experimental results, but here we simply assign the middle layer in Fig. 7(c) as the fourth QL because the deposited amount of Mn is 5 ML. Upon further annealing of 30 min, the surface morphology exhibited a significant change. That is, the layered structure with discrete heights changed to rather even surfaces in Figs. 7(b) and 7(d). Along a solid line in Fig. 7(d), a profile in Fig. 7(f) does not exhibit the discrete layered structure as seen in Fig. 7(e). In Fig. 7(f), near the center along the profile a rather steep peak appears and gradually goes down by about 3 Å toward right-hand side, despite the region should show a flat profile because of the same layer. The line profile in Fig. 7(f) leads us to denote the morphology of Fig. 7(d) as a wavy surface structure. We discuss the morphology change upon annealing below.

V. FORMATION PROCESSES OF MnSi

In this section, we discuss formation processes of the MnSi ultrathin films based on the findings in the preceding section. Figure 8 represents schematic illustrations of the grown MnSi ultrathin films on Si(111) at 1.5, 3, and 5 ML of Mn deposition followed by annealing at 250 °C. At 1.5 ML deposition followed by subsequent annealing for 30 min, two levels of Si surfaces are observed as seen in Fig. 3(b): the survived original (7×7) surface regions (nonreacted regions) and the lower "2×2" regions where 1 BL of the original surface has been removed [see Fig. 8(a)]. As noted

above, we denote the removed regions craters. Here, it is emphasized that the MnSi 2D islands of 1 QL have never been observed and that the MnSi thin films grow with a thickness unit of 1 QL after 2 QL formation. We suggest that the first QL formed on Si(111) is so active that the second QL covers simultaneously the first one. 2 QLs are the minimum thickness for the initial epitaxial growth of the MnSi films. Therefore, the 2 QL MnSi 2D islands are formed (together with 3 QLs) in the case of 1.5 ML Mn as shown in Fig. 8(a). For the formation of 2 QLs, Mn atoms with $2\times\frac{4}{3}=2.67$ ML gather locally upon annealing, and the same coverage of Si atoms has to exist there in order to form a 2 QL MnSi 2D island. The top BL provides 2.08 ML of Si atoms in the on-site reaction with Mn atoms and the rest of Si atoms are supplied from the surrounding nonreacted top BL leaving craters.

In the case of 3 ML Mn, sufficient amount of Mn atoms is deposited for covering an entire surface with the 2 QL MnSi films. Since whole top BL is used in the on-site reaction, deep holes down to the second and the third BLs are created. Necessary amount of Si to form the 2 QL MnSi films $[(2.67-2.08)=0.59$ ML] is supplied efficiently through the holes. Most surfaces of the MnSi films of 2 QLs are atomically flat as typically shown in Fig. 6. Thus, it is understood why the flat MnSi ultrathin films are formed on the entire surface at ~3 ML-Mn deposition. The interface between the MnSi and Si substrate would be rather smooth as shown in Fig. 8(b) except for holes.

At 5 ML-Mn deposition followed by annealing at 250 °C for 5 min, Si atoms of 5 ML are used for the reactive growth of the MnSi. Besides Si atoms of 2.08 ML in the top BL, about 3 ML (rather large amount) should be supplied from deeper BLs of the substrate. For this supply, many large holes are created as seen in Fig. 7(c) and a schematic illustration is depicted in Fig. 8(c). The surface is not so flat as the case of 3 ML-Mn deposition (cf. Fig. 6) and exhibits a layered structure with discrete heights as seen in Fig. 7(c). The wavy surface structure in Fig. 7(d) appears after prolonged annealing as mentioned above. Its origin is not clear at this stage. One possible reason is a collapse of "caves" which are formed by mining of deep Si layers. As mentioned above, necessary amount of Si atoms are supplied through the holes. Because the amount is significant, the mining toward lateral directions might be necessary and caves are formed around the holes as illustrated in Fig. 8(c). These caves having 1 BL height would collapse upon prolonged annealing. Then, the surface exhibits the wavy structure in Fig. 7(f). The decrease in the height seen in Fig. 7(f), ~3 Å might support the above possibility.

VI. CODEPOSITION OF Mn AND Si

It has become clear in the present experiments that the surface morphology including the holes and the craters is strongly affected by the processes of the supply of Si atoms. Even if 8/3 ML of Mn is deposited (corresponding to the exact amount for 2 QLs), the top BL can supply only 2.08 ML of Si. Then, 0.59 ML of Si should be supplied through the holes. Suppose that 2.08 ML Mn is deposited, whole Si atoms in the top BL can react to form the 2 QL MnSi. However, the craters are formed on the surfaces according to a balance of masses of Mn and Si (see Fig. 4 of Ref. 15). Therefore, it seems impossible to form completely flat surfaces of the MnSi films by the process of Mn deposition and subsequent annealing.

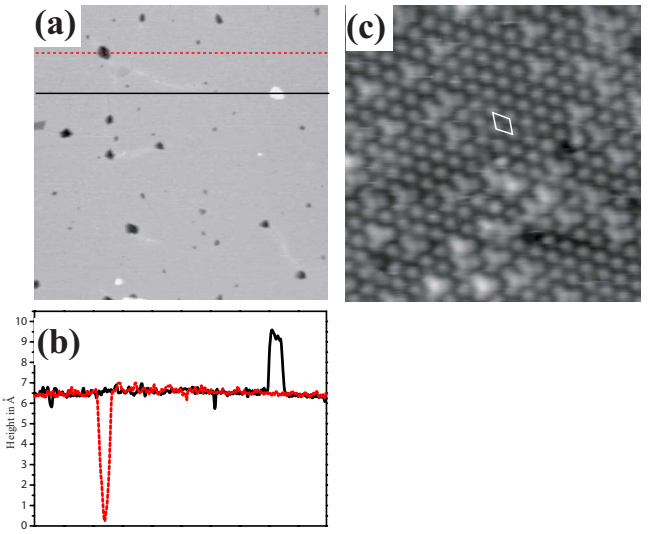

FIG. 9. (Color online) CC mode image of the MnSi surface formed by codeposition followed by annealing at 250 °C (150×150 nm^2). (b) Profiles along solid and dotted lines in (a). (c) A magnified image (10×10 nm^2) of the smooth surface, where the $(\sqrt{3}\times\sqrt{3})$R30° arrangement of protrusions is seen as outlined.

By using LEED, Magnano *et al.*[17] reported previously an improvement of the surface quality of films by means of simultaneous deposition of Mn and Si. Starke *et al.*[18] also found that the quality of LEED patterns of iron silicides was improved by simultaneous deposition of Fe and Si on the Si(111) surface followed by annealing. However, there is no STM report on the improvement of surface morphology by the codeposition. Here, we have successfully prepared highly smooth surfaces of the crystalline MnSi thin films by dosing Si atoms in addition to Mn atoms as shown in STM images (CC mode) of Fig. 9(a). A small number of tiny holes are found but almost entire surface (98%) exhibits an atomically flat MnSi film. Profiles along lines in Fig. 9(a) are depicted in Fig. 9(b). An enlarged image of Fig. 9(c) exhibits the $(\sqrt{3}\times\sqrt{3})$R30° arrangement of protrusions, where some unknown adatoms exist.[12] This smooth surface is prepared as follows: 1.5 ML Si was deposited first; then the deposition of Mn of 3 ML was carried out; finally 1.5 ML Si was deposited again. Then, the sample was annealed at 250 °C for 5 min. In Fig. 9(a), the smooth surface is the second QL of the MnSi because both deposited amounts of Si and Mn are 3 ML, which is close to 8/3 ML required for 2 QLs. Since Si atoms are supplied from outside of the sample, Mn atoms on the surface can react with adsorbed Si atoms to form the MnSi without making holes. Thus, it is confirmed that the formation of the holes on the epitaxially grown MnSi thin films formed by Mn deposition (3 and 5 ML) and subsequent annealing is caused by the necessity of supply of Si atoms to saturate Mn atoms to form the MnSi.

VII. SUMMARY

Mn adsorption followed by annealing at a relatively low temperature of 250 °C on the Si(111)-(7×7) has been studied by STM as well as by LEED and AES. The B20-type structure of the MnSi is formed in processes of the reactive epitaxial growth. Morphological changes in the crystalline MnSi ultrathin films have been investigated by mainly STM for Mn coverage of 1.5, 3, and 5 ML. We summarize important features of the MnSi growth obtained in the present experiments: (1) the minimum thickness of the grown MnSi 2D films is 2 QLs as observed at 1.5 ML-Mn deposition; (2) the MnSi grows with the thickness unit of 1 QL of the B20 structure after the initial 2 QLs formation; (3) Si atoms in the top BL of the original Si(111)-(7×7) surface are used to produce the MnSi 2D islands leaving craters as evidenced at 1.5 ML-Mn deposition; (4) at 3 ML-Mn deposition, the surface is almost flat in atomic scale and mostly covered by 2 QLs of the MnSi; (5) holes going down to the bare Si are created at 3 and 5 ML-Mn depositions; (6) and at 5 ML-Mn deposition, the surface exhibiting discrete layered structures changes to a wavy structure upon prolonged annealing.

Based on the above features, it is noted first that a characteristic mode of crystal growth for compound formation is found in the solid-on-solid system. That is, the crystalline MnSi ultrathin films grow epitaxially as 2 QLs at the initial growth, and the films further grow in a mode of 1-QL-by-1-QL after the initial 2 QLs formation. The reason for the occurrence of this specific growth mode in the epitaxial MnSi ultrathin films is not clear. Theoretical studies are required to solve the problems. Next, we summarize formation processes at each deposition amount of Mn. At 1.5 ML of Mn, the top BL with Si adatoms of the Si(111)-(7×7) reconstruction (2.08 ML) is provided on site for the MnSi formation, while the rest of Si is supplied from nonreacted Si surface leaving craters. At 3 ML, the MnSi covers the entire surface since an appropriate amount of Mn is deposited for the almost complete formation of the 2 QLs MnSi. Additionally necessary amount of Si atoms is supplied by making holes. Thus, most surfaces are atomically flat, although small holes and 2D islands of 3 QLs coexist. At 5 ML, uneven surfaces of the MnSi are formed with holes at short annealing time. After prolonged annealing, the layered structure with discrete heights drastically changes to rather even surfaces. Thus, we found that surface morphology is strongly dependent on the Si supply processes. In order to get more smooth MnSi layers on Si(111), we adopted the procedure of the codeposition of Si and Mn. Anomalously smooth surfaces of ultrathin films of the MnSi are coherently grown, where very low density of holes and 2D islands (only 2% of the surface) is demonstrated by STM. Thus prepared MnSi ultrathin films are expected to have smooth interface structures and therefore their application to the Si-based spintronics is highly hopeful.

ACKNOWLEDGMENTS

This work was supported by the Grants-in-Aid for Scientific Research under Grants No. 19340083, No. 18.06750, and No. 18.9776. P.K. appreciates support from the JSPS.

*tochihar@mm.kyushu-u.ac.jp

[1] G. A. Prinz, Science **282**, 1660 (1998).
[2] S. A. Wolf, D. D. Awschalom, R. A. Buhrman, J. M. Daughton, S. von Molnár, M. L. Roukes, A. Y. Chtchelkanova, and D. M. Treger, Science **294**, 1488 (2001).
[3] H. J. Zhu, M. Ramsteiner, H. Kostial, M. Wassermeier, H.-P. Schönherr, and K. H. Ploog, Phys. Rev. Lett. **87**, 016601 (2001).
[4] M. Ramsteiner, H. Y. Hao, A. Kawaharazuka, H. J. Zhu, M. Kästner, R. Hey, L. Däweritz, H. T. Grahn, and K. H. Ploog, Phys. Rev. B **66**, 081304(R) (2002).
[5] M. Zwierzycki, K. Xia, P. J. Kelly, G. E. W. Bauer, and I. Turek, Phys. Rev. B **67**, 092401 (2003).
[6] A. Kawaharazuka, M. Ramsteiner, J. Herfort, H.-P. Schönherr, H. Kostial, and K. H. Ploog, Appl. Phys. Lett. **85**, 3492 (2004).
[7] M. Hortamani, P. Kratzer, and M. Scheffler, Phys. Rev. B **76**, 235426 (2007).
[8] S. Azatyan, M. Hirai, M. Kusaka, and M. Iwami, Appl. Surf. Sci. **237**, 105 (2004).
[9] S. G. Azatyan, M. Iwami, and V. G. Lifshits, Surf. Sci. **589**, 106 (2005).
[10] D. Y. Wang, H. Y. Wu, L. J. Chen, W. He, Q. F. Zhan, and Z. H. Cheng, J. Phys.: Condens. Matter **18**, 6357 (2006).
[11] M. M. R. Evans, J. C. Glueckstein, and J. Nogami, Phys. Rev. B **53**, 4000 (1996).
[12] A. Kumar, M. Tallarida, M. Hausmann, U. Starke, and K. Horn, J. Phys. D **37**, 1083 (2004).
[13] T. Nagao, S. Ohuchi, Y. Matsuoka, and S. Hasegawa, Surf. Sci. **419**, 134 (1999).
[14] T. Shirasawa, S. Higashi, H. Tochihara, W. Voegeli, and T. Takahashi, 64th Annual Meeting Abstracts of the Physical Society of Japan, 2009, Vol. 64, 4–871.
[15] S. Higashi, Y. Ikedo, P. Kocán, and H. Tochihara, Appl. Phys. Lett. **93**, 013104 (2008).
[16] S. Higashi, T. Ohshima, S. Mizuno, and H. Tochihara, Surf. Sci. **600**, 591 (2006).
[17] E. Magnano, E. Carleschi, A. Nicolaou, T. Pardini, M. Zangrando, and F. Parmigiani, Surf. Sci. **600**, 3932 (2006).
[18] U. Starke, W. Weiss, M. Kutschera, R. Bandorf, and K. Heinz, J. Appl. Phys. **91**, 6154 (2002).